Journal of Applied Polymer Science

Surface Molecularly Imprinted Polymer Prepared by Reverse Atom Transfer Radical Polymerization for Selective Adsorption Indole

Yang Cao, Lukuan Liu, Wanzhen Xu, Xiangyang Wu, Weihong Huang
School of the Environment and Safety Engineering, Jiangsu University, Zhenjiang 212013, China
Correspondence to: W. Z. Xu (E-mail: xwz09@ujs.edu.cn) and X. Y. Wu (E-mail: wuxy@ujs.edu.cn)

ABSTRACT: The preparation of indole molecularly imprinted polymers (indole-MIPs) using 4-vinylpyridine as functional monomer, silica gel as matrix were used to adsorb indole from fuel oil specifically. The reverse atom transfer radical polymerization (RATRP) technology was introduced to prepare the surface molecularly imprinted polymers, and the precipitation polymerization was adopted in the preparation process. The obtained indole-MIPs were characterized by nitrogen adsorption, Fourier transform infrared spectrometry and scanning electron microscopy. The results show that indole-MIPs were provided with the larger surface areas and more pores. The adsorption capacity of indole-MIPs was 31.80 mg g^{-1} at 298 K, and the adsorption equilibrium was reached in a short time. The adsorption process was spontaneous by thermodynamic analysis, and an appropriate decrease in temperature could enhance the adsorption capacity. The adsorption process obeyed pseudo-second-order kinetic model by kinetics analysis. The isotherm analysis results show that both Langmuir and Sips equations were suitable to experimental data. The selective adsorption and reusable performance of indole-MIPs were favorable. © 2014 Wiley Periodicals, Inc. J. Appl. Polym. Sci. **2014**, *131*, 40473.

KEYWORDS: adsorption; kinetics; molecular recognition; radical polymerization

Received 20 September 2013; accepted 18 January 2014
DOI: 10.1002/app.40473

INTRODUCTION

Many kinds of nitrogenous compounds contained in fuel oil could cause a poor quality and low stability.[1] Large quantities of the harmful gas, such as nitric oxide (NO), nitrogen dioxide (NO_2) is emitted when the fuel oil products are used, and it would lead to the serious environmental contamination. The NO in the air could harm human health and compromise the quality of life.[2] The NO_2 contributes to the formation of the acidic fog and acid rain. Furthermore, the nitrogen oxides and hydrocarbon in atmospheric environment could lead to photochemical smog under intense ultraviolet radiation.[3,4] The nitrogenous compounds of fuel oil are divided into basic nitrogen and nonbasic nitrogen.[5] Some methods for removing the basic nitrogen such as hydrodenitrogenation (HDN), acid extraction, and ion exchange, etc[6–8] have achieved notable results. But these measures are not effective for the removal of harsh nonbasic nitrogen such as indole and its derivative. Therefore, the advanced denitrogenation has become a new and fascinating area of research in recent years.

Recently, molecular imprinting technology (MIT) is a promising way to prepare molecularly imprinted polymers (MIPs) with stability, low cost, and predetermined recognition ability to target molecular.[9–11] And the MIPs with the characteristics of desired selectivity and physical robustness have been widely applied in different areas, such as solid-phase extraction, biomimetic catalysis and drug development and so on.[12–16] Functional monomer, template, crosslinker, and initiator are contained in imprinting system where functional monomer interacts with template via noncovalent, such as hydrogen bonds, ionic, and electrostatic interaction, intermolecular force, etc.[11,17–19] In the presence of crosslinker and initiator, the polymerization is carried out, and then the polymer is prepared successfully. After the removal of template from the obtained polymer network, the molecularly imprinted binding sites matched with the shape, size and functional group of the template are achieved. However, the traditional molecular imprinting technology has many drawbacks, such as heterogeneous sites, limitation of adsorption, and unfavorable kinetics of the adsorption process.[20–22] Therefore, the surface molecular imprinting technology is successfully introduced to overcome these limitations. The MIPs prepared by surface molecular imprinting technology own the larger surface area and more poles, not only the nice selectivity, but also the high adsorption capacity and fast mass transfer have sown.[23,24]

The bulk polymerization, suspension polymerization, precipitation polymerization, and emulsion polymerization are included in the preparation methods of MIPs.[25–28] Most of reported MIPs have been synthesized by the bulk polymerization.

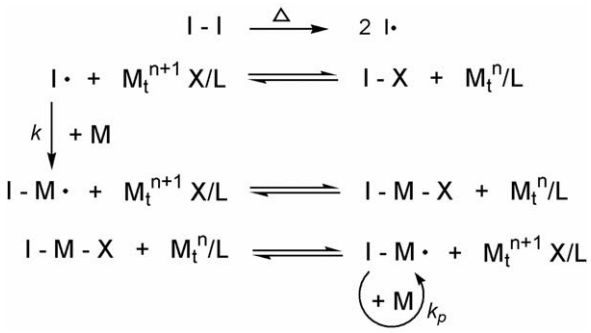

Figure 1. Schematic illustration of RATRP.

Although this method possesses the advantage of easy preparation for small amounts of MIPs, the polymerization process is time consuming,[29] and the obtained particles are irregular. At the same time, the less available quantity of MIPs is shown. For suspension polymerization, the cost of preparation is increased due to the requirement of large amount of surfactant. Therefore, the interaction of functional monomer with template is subjected to interference.[30] Among of them above, precipitation polymerization with the characteristics of easy operation and no need for any surfactant has been proved very versatile for the preparation of MIPs microspheres.[31–33]

It has been widely known that atom transfer radical polymerization (ATRP) with many advantages was a powerful way to prepare MIPs.[34–36] The "living"/controlled radical polymerization shows some merits, such as simple process, controlled molecular weight, and narrow distribution. The halogen atoms on terminal of polymers could be easily transformed into other functional groups.[37] However, the ATRP method has two drawbacks: the halides which serve as initiator are poisonous and not easily handled. Furthermore, the catalysts M_t^n/Lx at the low valence state are easily oxidized by air.[38] The development of reverse atom transfer radical polymerization (RATRP) has successfully overcome these disadvantages. The RATRP[39] uses a conventional radical initiator instead of *R–X*, and comparatively stable higher oxidation state transition metal compounds are adopted. The theory of RATRP is illustrated in Figure 1.[40]

At present, many studies reported the preparation of molecularly imprinted polymers, but less reports about the synthesis and application of indole molecularly imprinted polymers (indole-MIPs). Because of these polymers with a high adsorption capacity, excellent selectivity and good reusability, they could be applied in many fields. However, we prepared the indole-MIPs and applied in removal of organic nitrogen indole from fuel oil. In this article, the RATRP was introduced into the surface molecular imprinting technique, and the precipitation polymerization was adopted to prepare the indole-MIPs. The indole-MIPs were synthesized on the silica gel particles surface, and indole as template, 4-vinylpyridine (4VP) was chosen as functional monomer, ethylene glycol dimethacrylate (EDGMA) as cross-linker azobisisobutyronitrile (AIBN) as initiator. The catalyst system was consisted of $CuBr_2$/2, 2′-dipyridyl. Meanwhile, the nonimprinted polymers (NIPs) were also synthesized. The morphology and structure of the prepared indole-MIPs and NIPs were characterized by nitrogen adsorption, Fourier transform infrared spectrometry and scanning electron microscopy analysis, respectively. Pseudo-first-order kinetic model, pseudo-second-order kinetic model, and Elovich equation were used to analyze adsorption kinetics of indole-MIPs and NIPs towards indole. The Langmuir, Freundlich isotherms model, and Sips equation were selected to explore the effect of concentrations on adsorption capacity. The thermodynamics analysis and selectivity test were applied to study the adsorption mechanism of indole adsorbed on to indole-MIPs and NIPs.

EXPERIMENTAL

Materials and Instruments

Silica gel, indole (98.5%) and 4-vinylpyridine (4VP, 99.5%) were purchased from Aladdin Reagent Co. 3-Metlylindole (98%), quinoline (99%), benzothiophene (BT, 99%), ethylene glycol dimethacrylate (EGDMA, 98%), azobisisobutyronitrile (AIBN, 99%), n-octane (AR) were received from Sigma-Aldrich Chemical Company. Tetradecane (99.9%) and acetone (AR) were obtained from Nanjing Union Silicon Chemical. $CuBr_2$ (AR), 2, 2′-dipyridyl (98%), MPS (97%), methanol (MeOH, AR), acetic acid (AcOH, AR), and ethanol (AR) were supplied by the Sinopharm Chemical Reagent.

NICOLET NEXUS 470 Fourier transform infrared spectrometry (FT-IR) was received from Thermoelectric (USA). Flowsorb II 2300 manufactured by Micromeritics Instrument Corporation, Norcross, GA. S-4800 field emission scanning electron microscopy (SEM) was obtained from Hitachi. Agilent 7890A Gas Chromatography (GC) contained a flame ionization detector was manufactured from Agilent.

Preparation of Indole-MIPs and NIPs by RATRP

Preparation of Modified Silica Gel. At first, silica gel particles were dipped into 10% HCl solution for 24 h, filtered and washed repeatedly by distilled water until the solution was neutral, and then dried in vacuum at 90°C. The pretreatment was to eliminate any surface contaminants, and a dense mass of hydroxyl groups was introduced on the silica gel particles surface. Then, the activated silica gel particles were modified with MPS in toluene under a constant temperature of 114°C with continuous stirring for 24 h. This reaction was carried out in order to introduce polymerizable double bonds. The modified silica gel (MPS@silica gel) was separated and washed with toluene, acetone, and ethanol in sequence and then dried under vacuum at 60°C.

Preparation of Indole-MIPs and NIPs

The polymerization was carried out into a round bottomed flask with 20 mL acetonitrile and 1 g obtained MPS@silica gel. Then, the template molecule indole (0.4 mmol) and functional monomer 4VP (1.6 mmol) were successively added. After ultrasonic processing for 10 min, the solution was saturated with dry nitrogen for 15 min to eliminate oxygen, and the flask was sealed under the nitrogen atmosphere. The prepolymerization of template and functional monomer happened and lasted for 4 h in the thermostatic oil bath. And then EDGMA (8 mmol), AIBN (0.1 mmol), $CuBr_2$ (0.15 mmol), and 2, 2′-dipyridyl

(0.2 mmol) were added into mixed solution. The polymerization was kept at 60°C for 24 h under the protection of nitrogen and without stirring. At last, the resulted mixture was filtered and washed with acetone and ethanol in sequence and dried under vacuum at 60°C. The template was removed from indole-MIPs by a mixed methanol/acetic acid solvent (9 : 1, v/v) for 72 h. Then the product was dried under vacuum at 60°C, and the indole-MIPs were obtained. In comparison, the nonimprinted polymers were prepared as a blank, but without the addition of template molecule.

Characterizations of the Prepared Indole-MIPs and NIPs

Flowsorb II 2300 was used to measure the specific area ($m^2\ g^{-1}$), the pore volume ($cm^3\ g^{-1}$) and pore diameter (Å) of indole-MIPs and NIPs. NICOLET NEXUS 470 FT-IR was applied to detect the spectral line of functional groups in each polymerization step with KBr as tableting between 4000 and 400 cm^{-1}. And the S-4800 field emission scanning electron microscopy was used to characterize the morphology of polymers.

Adsorption Capacity Tests of Indole-MIPs and NIPs

Test of Adsorption Kinetics. The adsorption kinetics was usually used to investigate the equilibrium time and the rate of indole adsorbed on to indole-MIPs and NIPs, respectively. All of the six groups tests have been performed in simulate oil (n-octane as solvent) containing indole (initial concentration of 300 mg L^{-1}). The parallel experiments were carried out at 298, 308, and 318 K, respectively. Specific operations as follows: firstly, 10 mg of indole-MIPs (NIPs) and 5 mL of simulate oil were added into centrifuge tubes, and then shaken in a vapor-bathing constant temperature vibrator at the preset temperatures for predetermined time intervals, respectively. After centrifuged, the concentrations of indole remaining in the supernatant for different time intervals were detected by GC. The adsorption capacity was calculated as follow eq. (1).

$$q_t = (C_0 - C_t)V/m \quad (1)$$

where q_t (mg g^{-1}) represents the adsorption ability of polymers at time t; C_0 and C_t are the concentrations of indole at initial and time t, respectively; V is the volume of simulate oil and m is the mass of indole-MIPs (NIPs).

Test of Adsorption Isotherm. For the purpose of exploring the effect of initial concentrations on adsorption capacity, the test of adsorption isotherms was explored in different initial concentrations simulate oil. At first, 10 mg of the indole-MIPs (NIPs) was added into test tubes containing 5 mL of simulate oil solution with concentration gradients (100–1000 mg L^{-1}) of indole. Then, the test tubes were respectively shaken in vapour-bathing constant temperature vibrators at the preset temperatures (298, 308, and 318 K) for 3 h. At last, centrifuging and taking the supernatant from tubes. GC was used to detect the concentrations of remaining indole. The equilibrium adsorption capacity was obtained according to the following eq. (2)

$$q_e = (C_0 - C_e)V/m \quad (2)$$

where q_e (mg g^{-1}) is the adsorption capacity of indole-MIPs (NIPs) and C_e (mg L^{-1}) is the equilibrium concentration of indole in simulate oil.

Test of Selective Adsorption. Indole and its analogues such as 3-metlylindole, quinoline and benzothiophene (BT) were chosen to test the selectivity of indole-MIPs and NIPs. The adsorption experiments were conducted in a mixed solution containing 300 mg L^{-1} of above substances. The operation process was similar to adsorption isotherms, and the adsorption conditions were allowed to conduct at 298 K for 3 h.

RESULTS AND DISCUSSION

Preparation of the Indole-MIPs

Silica gel was selected as supporter own to the large specific area, and the polymer grafted on the silica gel particles surface could possess a high adsorption capacity. The silica gel particles were activated by HCl and modified by grafting MPS, so the polymerizable double bonds were introduced on the silica gel particles surface to carry out the polymerization reaction. The 4VP was picked as the functional monomer based on the hydrogen bond formed between 4VP and indole, and multiple hydrogen-binding sites could be provided. Furthermore, the mol ratio of functional monomer and template molecule of 4 : 1 was chosen in the polymerization process.[41–43] The EGDMA was chosen as cross-linker, acetonitrile as solvent, and the polymerization was initiated by the AIBN, and transition metal complex (Cu^{2+}/2, 2′-dipyridyl) in its higher oxidation state was selected as catalyst. The polymerization system we adopted combined the surface MIT and RATRP, not only overcome some drawbacks such as the limitation of adsorption and imprinting sites embedded, but also solve the problem of poisonous catalyst and strict requirement for nitrogen in ATRP system. Meanwhile, some merits such as controlled molecular weight and narrow distribution of the "living"/controlled radical polymerization were realized. Furthermore, the precipitation polymerization was introduced to simply the polymerization operation.

The schematic illustration of polymerization was shown in Figure 2.

Structural Characteristics of Indole-MIPs and NIPs

Nitrogen Adsorption Analysis. Brunauer–Emmett–Teller (BET) and Barrett–Joyer–Halendal (BJH) models were used to test structural characteristics of indole-MIPs and NIPs. The obtained analysis results were listed in Table I. The pore properties values of indole-MIPs were all greater than NIPs. It was attributed to more pores left by the elution of template indole. So the indole-MIPs were more accessible to indole, and benefited to the conduction of the interaction.

Infrared Spectrum Analysis. In Figure 3, spectral line *a*, *b*, *c*, and *d*, respectively, were IR spectra of silica gel, activated silica gel, MPS-silica gel and indole-MIPs. In spectral line a, the characteristic adsorption peak of Si-O was shown at 1102 cm^{-1}. Compared with spectral line *a*, hydroxyl characteristic vibration adsorption peak appeared at 3421 cm^{-1} in spectral line *b*. The hydroxyl group introduced on the silica gel surface proves that the silica gel was successfully activated. Furthermore, the band at around 2977 cm^{-1} was assigned to the stretching vibration of —CH_2— or —CH_3—, and the C=O stretching vibration absorption peak appeared at about 1728 cm^{-1} in spectral line c.

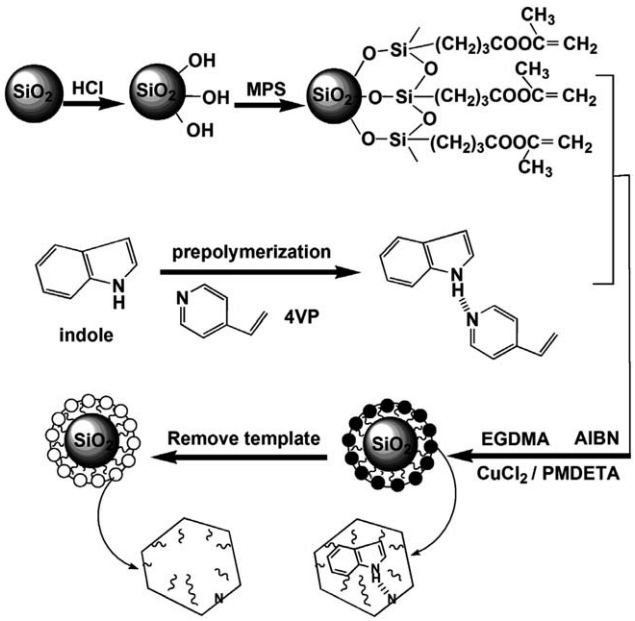

Figure 2. Schematic for the preparation of indole-MIPs

It indicates that the MPS has been grafted on the activated silica gel. In spectral line d, the adsorption peak at 1390 cm^{-1} was generated by —CH_3 characteristic absorption, and the —CH_2—CH_2— bending vibration absorption peak was shown at 1458 cm^{-1}. The C═N deformation vibration peak appeared at about 1601 cm^{-1}. In addition, the hydroxyl characteristic vibration adsorption peak was weak and the C═O stretching vibration absorption peak was strong. It proves that 4VP was successfully cross-linked on the modified silica gel surface. Overall, the absorption peaks of indole-MIPs prove that the polymers were successfully grafted on the silica gel surface.

SEM Analysis. The SEM images of indole-MIPs and NIPs were shown in Figures 4(a,b) respectively. Compared with the SEM image of NIPs, indole-MIPs owned more amounts of pores and larger surface areas. At the same time, the surface of indole-MIPs was rougher than that of NIPs.

Characterization of Adsorption Performance

Analysis of Adsorption Thermodynamics. These parameters: the standard free energy change (ΔG°), the standard enthalpy change (ΔH°), and the standard entropy change (ΔS°) were used to reflect the thermodynamic characteristics of the adsorption processes of indole-MIPs and NIPs.[44,45] They could be calculated by eqs. (3) and (4).

$$\ln K_c = -\Delta H^\circ / \mathrm{RT} + \Delta S^\circ / R \quad (3)$$

Table I. Pore Properties of Indole-MIPs and NIPs

Polymers	Specific area ($m^2\ g^{-1}$)	Pore volume ($cm^3\ g^{-1}$)	Pore diameter (Å)
Indole-MIPs	256.296	0.486	28.880
NIPs	248.985	0.451	28.793

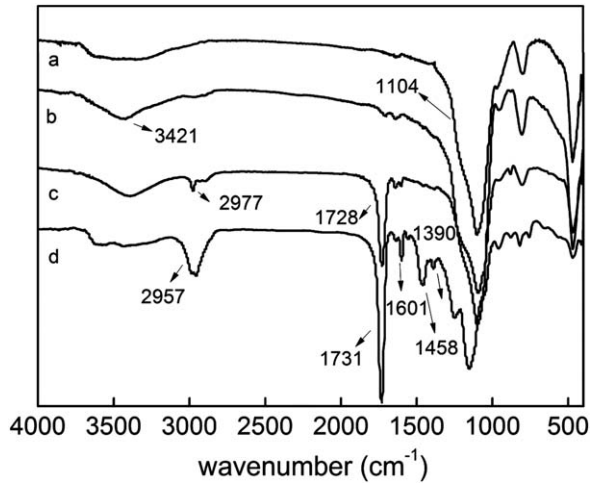

Figure 3. FT-IR spectra of silica gel (a), activated silica gel (b), MPS@silica gel (c), and indole-MIPs (d).

$$\Delta G^\circ = \Delta H^\circ - T\Delta S^\circ \quad (4)$$

where K_c is an distribution constant (mL g^{-1}) and can be obtained by plotting $\ln(q_e/C_e)$ versus q_e and extrapolating q_e to zero, and the values of K_c are given by the intercept of the straight line; T is the absolute temperature (K); R is the gas constant (8.3145 J mol^{-1} K−1).

The experiments were carried out in different concentrations of indole (range from 100 to 1000 mg L^{-1}) at 298, 308, and 318 K, respectively. The values of ΔH°, ΔS°, and ΔG° are reported in Table II.

As shown in Table II, a negative value of ΔG° indicates the feasibility of the process and the spontaneous nature of the adsorption process of indole-MIPs towards indole within the temperature range. And a negative value of ΔH° reflected the exothermic adsorption process. Thus, the decreasing temperature provided a more favorable adsorption, and the conclusion has been verified by isotherm experiment. For the NIPs, the adsorption process was also spontaneous by a negative ΔG°. However, the endothermic adsorption process was shown by a positive value of ΔH°. It was different from the adsorption of indole-MIPs towards indole. Meanwhile, the positive values of ΔS° of the two adsorption processes indicate the increase in randomness of the solid/solution interface during the adsorption process, so the higher affinity towards indole were obtained at a high concentration. Compared with ΔS°, the indole-MIPs increased more randomly than the NIP, thus the adsorption is more easily happened on indole-MIPs. Compared with ΔG° for the adsorption of polymers towards template, the spontaneous adsorptive forces were stronger.

Analysis of Adsorption Kinetics. To clarify the adsorption mechanism of adsorbents towards indole, the pseudo-first-order, pseudo-second-order kinetics models[46,47] and Elovich equation[48] were used to fit the experimental data. And the three kinetics models were expressed by eq. (5–7):

$$\log(q_e - q_t) = \log q_e - k_1 t/2.303 \quad (5)$$

$$t/q_t = 1/k_2 q_e^2 + t/q_e \quad (6)$$

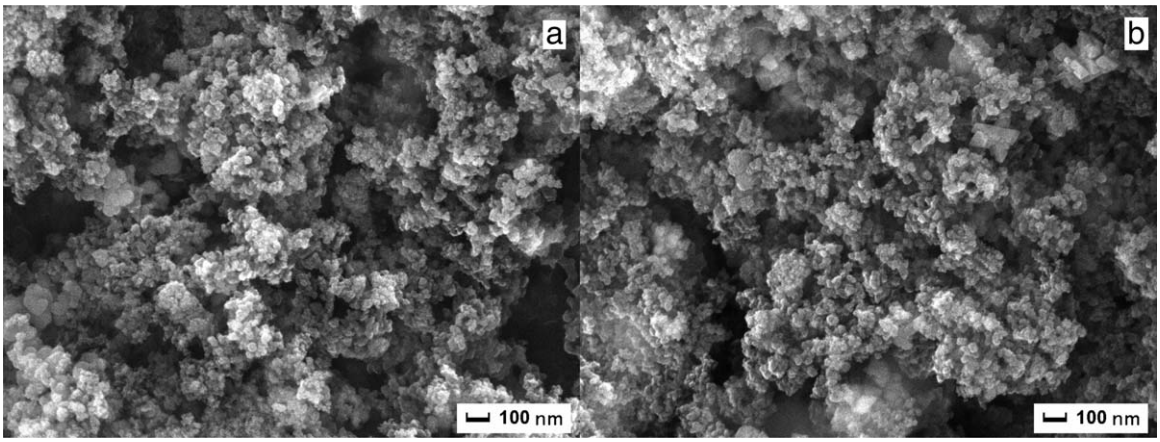

Figure 4. SEM images of indole-MIPs (a) and NIPs (b).

$$q_t = \ln(ab)/b + \ln t/b \quad (7)$$

where q_e (mg g^{-1}) and q_t (mg g^{-1}) are amount of adsorbed indole at equilibrium and time t, respectively; k_1 and k_2 respectively are the adsorption rate constants of pseudo-first-order and pseudo-second-order kinetics models; $q_{e,exp}$ and $q_{e,cal}$ are experimental and calculated values of bound indole, respectively; a represents the initial adsorption rate and b is a constant related to the surface coverage.

The experimental results, fitting curves of three models and parameters were shown in Figure 5 and Table III.

As shown in Figure 5(a), in the adsorption initial stage, a rapid increase in adsorption capacity was shown, and the adsorbance had a linearity relation with adsorption time. Subsequently, the adsorption capacity increased slowly until the adsorption equilibrium was reached. The adsorption rate decreased with time due to an increase in the adsorbent surface coverage. The adsorption equilibrium of indole-MIPs towards indole was achieved in 90 min even at different temperatures. Furthermore, the indole-MIPs showed a high adsorption capacity, and the maximum adsorption capacity was 31.80 mg g^{-1}. It implies that it was more conductive to the interaction by existing pore structure, and different temperatures had little effect on the adsorption equilibrium time. For the NIPs, the interaction time of adsorption equilibrium was absolutely reduced. However, the adsorption capacity of NIPs at equilibrium was only 15.00 mg g^{-1} shown in Figure 5(b). It is perceived that indole-MIPs were provided with the higher affinity to indole. The high affinity was not only due to hydrogen bond between target and functional monomer, but also electronic inductive effect, conjugative effect provided more possibilities to adsorption of binding sites.

As shown in Table III, compared with the pseudo-first-order kinetics model and Elovich equation, the pseudo-second-order kinetics model was more suitable to experimental data of indole-MIPs towards indole. The correlation coefficients (R^2) of three data sets were above 0.99. The adsorption behavior of NIPs was also in line with the pseudo-second-order model. Generally, the pseudo-second-order model could explain the adsorption mechanism better, because it was set up on the whole range of the adsorption equilibrium time. The initial adsorption rate of indole-MIPs towards indole was affected slightly by temperature. So, it was easy to speculate that the chemical adsorption was main to indole-MIPs towards indole, and the physical adsorption might be also concluded in the adsorption process.

Table II. Thermodynamic Parameters for the Adsorption Process of Indole-MIPs and NIPs Towards Indole

		Indole-MIPs			NIPs		
Kinetic models		298 K	308 K	318 K	298 K	308 K	318 K
	$q_{e,exp}$ (mg g^{-1})	31.798	28.896	23.697	9.811	12.979	14.979
Pseudo-first-order	$q_{e,cal}$ (mg g^{-1})	30.842	27.671	22.672	9.347	12.572	14.467
	k_1 (min^{-1})	0.0796	0.0812	0.0767	0.0891	0.0811	0.0842
	R^2 (nonlinear)	0.9475	0.9045	0.8805	0.8435	0.9385	0.9162
Pseudo-second-order	$q_{e,cal}$ (mg g^{-1})	32.939	29.604	24.306	9.9581	13.407	15.387
	k_2 (mg g^{-1} min^{-1})	0.0042	0.0047	0.0053	0.0158	0.0106	0.0098
	R^2 (nonlinear)	0.9907	0.9916	0.9949	0.9946	0.9822	0.9768
Elovich	a (mg g^{-1} min^{-1})	173.29	146.59	84.006	95.512	83.993	135.59
	b (g mg^{-1})	0.2855	0.3147	0.3670	1.0059	0.7156	0.6474
	R^2 (nonlinear)	0.8219	0.8610	0.8935	0.8975	0.8151	0.8171

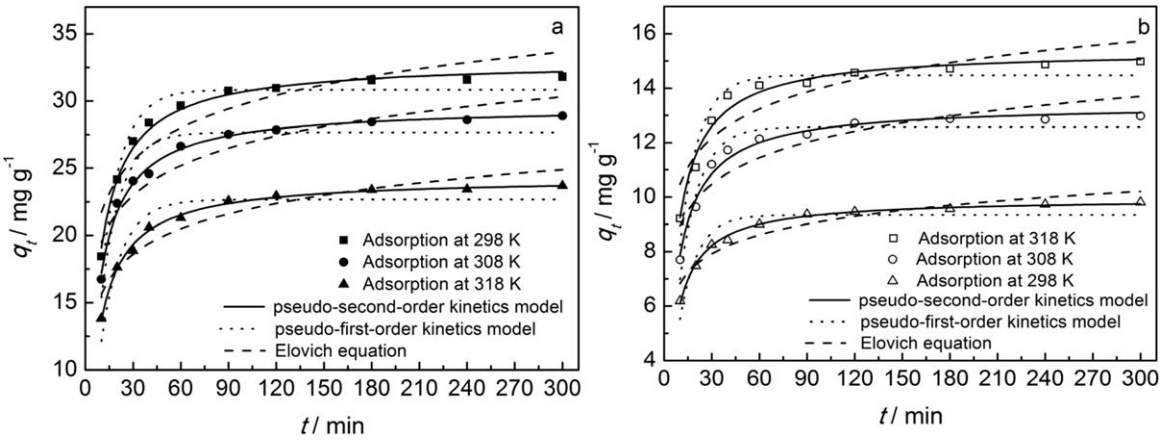

Figure 5. Kinetic adsorption curves of idole-MIPs (a) NIPs (b) towards indole at 298, 308, and 318 K, respectively.

Analysis of Adsorption Isotherms. The adsorption isotherms properties of adsorbents were analyzed by two-parameter isotherm models: Langmuir and Freundlich isothermal equations.[46,48] The two equations were given as eq. (8) (9), respectively. The former was used to describe monolayer adsorption and the latter as an empirical equation was used to describe adsorption process. The three-parameter isotherm models: Sips equation[48] was also picked to analyze the experimental data, and the equation was expresses by eq. (10). And the fitting curves and analysis results were shown in Figure 6 and Table IV.

$$C_e/q_e = C_e/q_m + 1/(q_m K_L) \quad (8)$$

$$\log q_e = \log C_e/n + \log K_F \quad (9)$$

$$q_e = q_{mS}(a_s C_e)^{1/ns}/(1+(a_s C_e)^{1/ns}) \quad (10)$$

where q_m (mg g^{-1}) is the maximum adsorption capacity of monolayer adsorption, and it can be obtained by calculation; K_L (L mg^{-1}) and K_F, respectively, are Langmuir and Freundlich constants; n is Freundlich constants related to temperature; a_s is a constant related to the adsorption energy. n_s is used to express the uniformity of adsorption.

As shown in Figure 6(a,b), with a certain amount of indole-MIPs, the adsorption capacity towards indole decreased with temperature increase. This performance was attributed to the interaction of hydrogen bond between indole and 4VP. The force of hydrogen bond was weak when the interaction occurred at a high temperature. However, the response of adsorption capacity to concentrations was different from that to temperatures. According to experimental results, the binding capacity increased with the increasing concentrations of indole. Nevertheless, the adsorption capacity of NIPs increased with the increasing temperatures and initial concentrations shown in Figure 6(b). The reason for this trend is that the physical adsorption was dominated in the adsorption process. Compared with NIPs, the indole-MIPs exhibited a distinctly favorable adsorption performance. Meanwhile, an appropriate decrease in temperature could enhance the adsorption process of indole-MIPs towards indole.

From Table IV, experimental results show that adsorption process of indole-MIPs towards indole was more consistent with Langmuir isothermal equation and Sips equation, so the monolayer adsorption for the adsorption process was proved. Sips equation was used to describe the adsorption on the inhomogeneous surface, and it combined Langmuir and Freundlich models. At high adsorbate concentration, it was equivalent to Langmuir equation, and it predicted the monolayer adsorption capacity. At low adsorbate concentration, however, it was equivalent to Freundlich model. In Sips equation, $1/n_s$ indicated the adsorption uniformity, and the closer the value to unity, the more uniform the surface of adsorbent was. From the Table IV, for indole-MIPs, the values of $1/n_s$ were close to unity. It proves that the adsorption of indole on to indole-MIPs surface was uniform, in other words, the uniform binding sites were

Table III. Kinetic Parameters of the Pseudo-first-order, Pseudo-second-order Kinetics Models, and Elovich Equation for the Adsorption of Indole-MIPs and NIPs Towards Indole

Polymers	T (K)	K_c	ΔG° (kJ mol^{-1})	ΔH° (kJ mol^{-1})	ΔS° (J mol^{-1} K^{-1})
	298	5.2460	−4.1067		
Indole-MIPs	308	4.9780	−4.1102	−4.0325	0.2328
	318	4.7350	−4.1113		
NIPs	298	3.9380	−3.3959		
	308	4.3380	−3.7578	5.4041	29.6162
	318	4.5150	−3.9856		

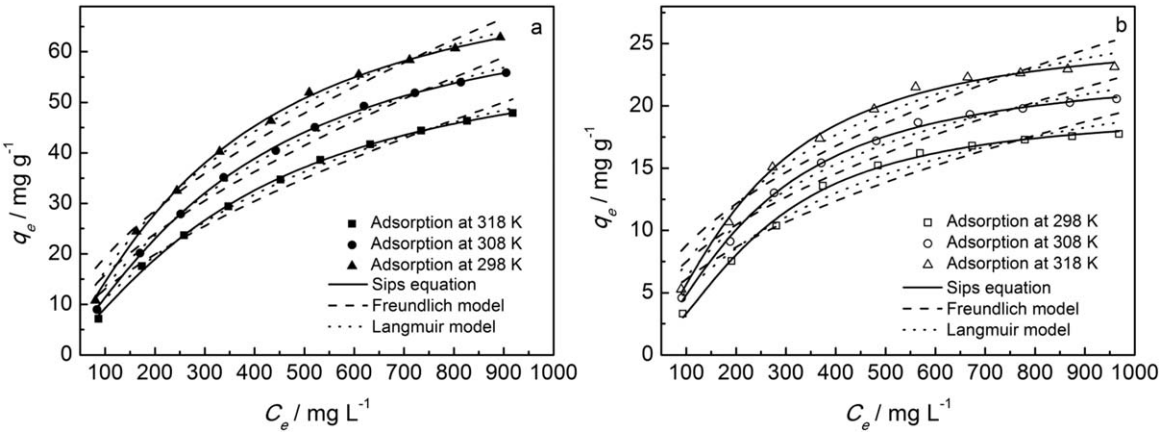

Figure 6. Adsorption isotherms and fitting curves of activated indole-MIPs (a) and NIPs (b) towards indole at different temperatures.

distributed on the indole-MIPs surface. However, the adsorption process of NIPs towards indole was more fitted with Freundlich isothermal model, and it indicates that the NIPs surface was nonuniform.

Analysis of Selective Adsorption. The parameters picked to judge selective adsorption of indole-MIPs and NIPs could be expressed by following equations. The distribution coefficients of indole, quinoline, 3-methylindole and BT were calculated by eq. (11).

$$K_d = q_e / C_e \tag{11}$$

where K_d (mL g^{-1}) is distribution coefficient; C_s (mg mL^{-1}) is the equilibrium concentration.

The selectivity coefficient indole-MIPs for indole towards its competitor (marked as B) could be calculated according to eq. (12).

$$k = K_d(\text{indole}) / K_d(B) \tag{12}$$

where k is the selectivity coefficient; B represents indole, quinoline, 3-methylindole and BT.

The relative selectivity coefficient k' could be calculated with eq. (13).

$$k' = k_{\text{indole-MIPs}} / k_{\text{NIPs}} \tag{13}$$

where k' is relative selectivity coefficient.

The parameters, such as K_d, k, and k' explained the binding capacity of indole-MIPs and NIPs towards indole, 3-methylindole, quinoline, and BT were summarized in Table V and illustrated by comparison in Figure 7(a). The structures of indole and its analogs were shown in Figure 7(b).

In the Figure 7(a), the results show that the adsorption capacity of indole-MIPs towards indole was higher than towards 3-methylindole, quinoline, and BT. Furthermore, the indole adsorbed on to indole-MIPs was more than on to NIPs. Meanwhile, the adsorption of both indole-MIPs and NIPs towards 3-methylindole was slightly higher than other two analogs, and the adsorbed BT was least.

In the mixed solution, the selective adsorption performance was well explained by the distribution K_d and selectivity coefficient k. From Table V, the K_d (indole) was obviously larger than K_d(3-methylindole, quinoline, and BT). Meanwhile, the value of k was greater than 1 entirely. Both of K_d and k enunciate that indole-MIPs had a better adsorption towards indole than towards 3-methylindole, quinoline, and BT. It means that

Table IV. Parameters of the Langmuir, Freundlich Isothermal Models, and Sips Equation

Isotherm models		Indole-MIPs			NIPs		
		298 K	308 K	318 K	298 K	308 K	318 K
Langmuir	k_L (L mg^{-1})	0.0020	0.0017	0.0015	0.0023	0.0027	0.0029
	q_{mL} (mg g^{-1})	99.877	95.150	83.790	27.013	29.574	33.038
	R^2 (nonlinear)	0.9932	0.9937	0.9938	0.9655	0.9796	0.9757
Freundlich	k_F	1.446	1.005	0.777	0.574	0.819	1.022
	n_F	1.776	1.671	1.633	1.952	2.082	2.141
	R^2 (nonlinear)	0.9644	0.9678	0.9689	0.9049	0.9216	0.9120
Sips	q_{ms} (mg g^{-1})	79.642	72.172	62.608	19.539	23.027	25.884
	a_s	0.0031	0.0028	0.0027	0.0041	0.0042	0.0045
	n_s	0.7772	0.7566	0.7558	0.5649	0.6443	0.6348
	R^2 (nonlinear)	0.9985	0.9993	0.9987	0.9959	0.9978	0.9960

Table V. Selective Recognition Parameters of Indole-MIPs and NIPs

	Indole-MIPs		NIPs		
Mixed solution	K_d	k	K_d	k	k'
Indole	103.578	-	63.915		
3-Metlylindole	43.894	2.360	39.774	1.607	1.468
Quinoline	25.708	4.029	23.928	2.671	1.508
BT	16.679	6.210	18.247	3.503	1.773

indole-MIPs towards indole had a selective adsorption. It could be attributed to spatial structure complementary and the hydrogen bond between template molecule indole and functional monomer 4VP. So the indole molecule could be easily identified by indole-MIPs. In addition, the imprinted sites obtained on the indole-MIPs surface were proved by aforementioned kinetic and isotherm experiments, and it was further tested and verified by selective adsorption experiment. In contrast, other analogs could not be distinguished accurately as a result of their sizes and special structures. For the same reason, compared with quinoline and BT, 3-methylindole with similar size and functional monomer adsorbed on to indole-MIPs increased significantly. The adsorption capacity of indole-MIPs towards BT was the least. The phenomenon could be explained by the fact that the force such as electrostatic attraction or intermolecular force between BT and indole-MIPs was weaker than hydrogen bond.

Relative to NIPs, the adsorption capacity was lower than that of indole-MIPs. Although the NIPs had no specific pores and binding sites, a little more adsorption capacity to indole than other analogs was shown. The reason is that the indole had specific combination with functional monomer 4VP.

In a word, the indole-MIPs towards indole were chemical adsorption via hydrogen bond interaction, and the physical adsorption was also included. But for NIPs, the physical adsorption was dominated, and the adsorption had no selectivity. The selective ability and imprinted binding sites of indole-MIPs were successfully obtained in the preparation process. Maybe a small number of specific binding sites were destroyed during the process of elution. There is no denying that the mechanism of indole-MIPs towards indole was not affected.

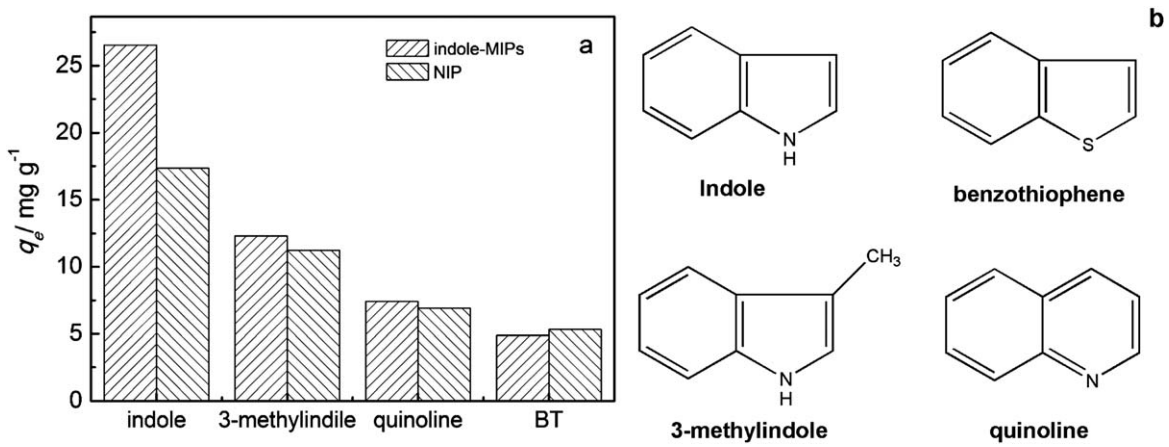

Figure 7. Effect of adsorption capacity towards indole, 3-methylindole, quinoline, and BT of indole-MIPs and NIPs.

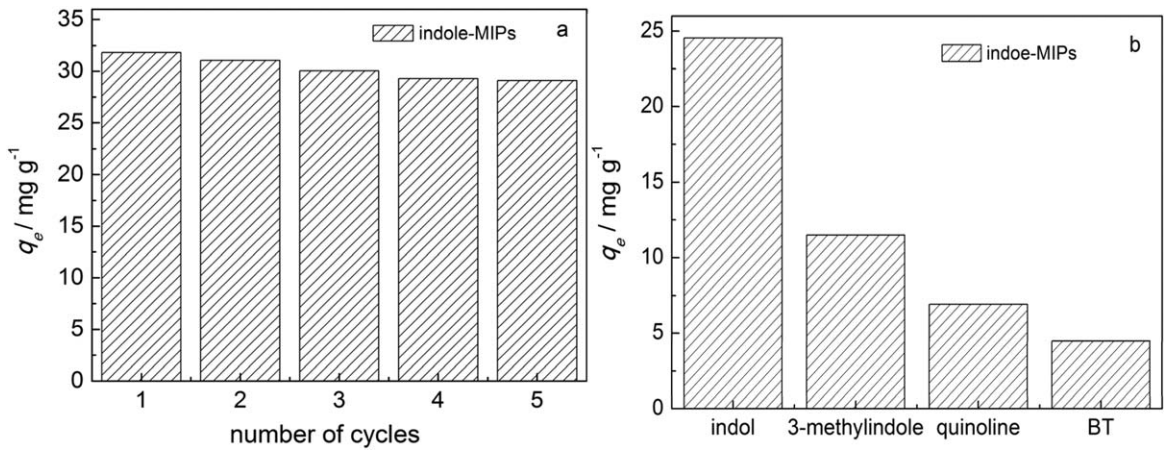

Figure 8. Regeneration of indole-MIPs for five cycles (a); selective adsorption of indole-MIPs towards indole and analogs in fifth cycle (b).

Regeneration of Indole-MIPs. To study the reusability and stability of indole-MIPs, the cycling experiments were carried out in the concentration of 300 mg L^{-1} of stimulate oil. The adsorption operation was similar to that of adsorption isotherms experiment, and 298 K was selected as the adsorption temperature for 3 h. The adsorption operation was repeated five times, and the mixture of methanol and acetic acid (9/1, V/V) was selected as an eluent. The results of five regeneration cycles were shown in Figure 8(a). After five cycles of adsorption and elution, the adsorption capacity of indole-MIPs declined by 8.6%. It indicates that the reusability of indole-MIPs prepared by RATRP was favorable.

The selective adsorption of indole-MIPs towards indole and other analogs in fifth cycle was also explored. The better adsorption for indole than 3-metlylindole, quinoline and BT was shown in Figure 8(b), and the calculated selectivity coefficients (k) were 2.31, 3.95, and 6.19, respectively. Compared with Table V, the value of k had no obvious decrease. This suggests that the excellent selectivity of indole-MIPs was maintained after five cycles.

CONCLUSION

In our work, we prepared a novel adsorbent (indole-MIPs) for selective recognition and adsorption of indole from fuel oil. The indole-MIPs were synthesized by a combination of the surface molecular imprinting technique and the reverse atom transfer radical polymerization. Meanwhile, the precipitation polymerization was adopted. The polymerization method overcome the limitation of adsorption and imprinting sites embedded, and the poisonous catalyst and strict requirement for nitrogen in ATRP system were worked out. The indole-MIPs were prepared with the high adsorption capacity (31.80 mg g^{-1}) as well as the short equilibrium time (90 min). The indole-MIPs could selectively remove the stubborn non-nitrogen indole and remain the stability of fuel oil. A series of characterization and experiments carried out to test the structural feature and performance of indole-MIPs and NIPs show that the indole-MIPs were provided with the larger specific areas and more pores than NIPs. For indole-MIPs, the adsorption process was spontaneous and exothermic by thermodynamic analysis, and an appropriate decrease in temperature could enhance the adsorption process. The pseudo-second-order model was obeyed by kinetics analysis. According to the isotherm analysis, both Langmuir and Sips equation were fitted to experimental data. Furthermore, the regeneration and selective adsorption of indole-MIPs were excellent even after five cycles. In conclusion, the preparation method was simple and effective to synthesize indole-MIPs, and the adsorption and selectivity performance of indole-MIPs was remarkable. Furthermore, the method used in field of selective adsorbing indole from fuel oil was available. The synthesis method and adsorption performance of indole-MIPs could be optimized and upgraded in the next stage.

ACKNOWLEDGMENTS

This work is subsidized by the National Natural Science Fund (No. 21106056, 21174057), Jiangsu Natural Science Fund of China (No. BK2011512), a Project Funded by the Priority Academic Program Development of Jiangsu Higher Education Institutions (PAPD), Senior Talent Foundation of Jiangsu University (No. 09JDG048), Scientific Research Foundation of Jiangsu University (No. Y11A133, Y10A035).

REFERENCES

1. Nwadinigwe, C. A.; Maduka, M. C. *Fuel* **1993**, *72*, 1139.
2. Karpuzoglu, Z.; Ahmed, A. *Nitric Oxide* **2006**, *15*, 177.
3. Kikugawa, K.; Kato, T.; Okamoto, Y. *Free Radic. Biol. Med.* **1994**, *16*, 373.
4. Takahashi, Y.; Miura T. *Toxicology* **1989**, *56*, 253.
5. Burchill, P.; Herod, A. A. *Fuel* **1983**, *62*, 20.
6. Nagai, M.; Masunaga, T. *Fuel* **1988**, *67*, 771.
7. Li, M.; Larter, S. R. *Org. Geochem.* **2001**, *32*, 1025.
8. Tokareva, L. N.; Kotova, A. V.; Bezinger, N. N.; Gal'pern, G. D. *Pet. Chem. USSR* **1968**, *8*, 146.
9. Liu, X.; Guan, Y. P.; Wang, Q.; Ren, X. F.; Yang, M. Z. *J. Appl. Polym. Sci.* **2012**, *126*, 1956.
10. Lee, S. C.; Chuang, F. L.; Tsai, Y. L.; Chen, H. *J. Polym. Res.* **2010**, *17*, 737.
11. Cela-Pérez, M. C.; Lasagabáster-Latorre, A.; Abad-López, M. J.; López-Vilariño, J. M.; Gónzalez-Rodríguez, M. V. *Vib. Spectrosc.* **2013**, *65*, 74.
12. Masqué, N.; Marcé, R. M.; Borrull, F. *Trend Anal. Chem.* **2001**, *20*, 477.
13. Abbate, V.; Bassindale, A. R.; Brandstadt K. F.; Taylor, P. G. *J. Catal.* **2011**, *284*, 68.
14. He, C. Y.; Long, Y. Y.; Pan, J. L.; Li, K.; Liu, F. *J. Biochem. Biophys. Methods* **2007**, *70*, 133.
15. Bures, P.; Huang, Y. B.; Oral, E.; Peppas, N. A. *J. Control Release* **2001**, *72*, 25.
16. Güney, O.; Cebeci, F. C. *J. Appl. Polym. Sci.* **2010**, *117*, 2373.
17. Ara, B.; Chen, Z. Y.; Shah, J. M.; Jan, M. R.; Ye, L. *J. Appl. Polym. Sci.* **2012**, *126*, 315.
18. Liu, Z. H.; Lv, Y. K.; Gao, J. G.; Li, X. L.; Zhai, X. F.; Zhao, J. H.; Xu, X. J. *J. Appl. Polym. Sci.* **2012**, *126*, 1247.
19. An, F. Q.; Gao, B. J.; Feng, X. Q. *J. Appl. Polym. Sci.* **2012**, *125*, 2549.
20. Niu, D. D.; Zhou, Z. P.; Yang, W. M.; Li, Y.; Xia, L.; Jiang, B.; Xu, W. Z.; Huang, W. H.; Zhu, T. Y. *J. Appl. Polym. Sci.* **2013**, *130*, 2859.
21. Liu, H. M.; Liu, C. H.; Yang, X. J.; Zeng, S. J.; Xiong, Y. Q.; Xu, W. *J. Anal Chim. Acta* **2008**, *628*, 87.
22. Liu, Y.; Liu, Z. C.; Gao, J.; Dai, J. D.; Han, J.; Wang, Y.; Xie, J. M.; Yan, Y. S. *J. Hazard Mater.* **2011**, *186*, 197.
23. Boonpangrak, S.; Prachayasittikul, V.; Bülow, L.; Ye, L. *J. Appl. Polym. Sci.* **2006**, *99*, 1390.
24. Sreenivasan, K. *J. Polym. Res.* **2001**, *8*, 197.
25. Nicolescu, T. V.; Sarbu, A.; Dima, S. Q.; Nicolae, C.; Donescu, D. *J. Appl. Polym. Sci.* **2013**, *127*, 366.
26. Yang, P.; Hou W. D.; Qiu H. D.; Liu, X.; Jiang, S. X. *Chin. Chem. Lett.* **2012**, *23*, 615.

27. Dai, J. D.; Pan, J. M.; Xu, L. C.; Li, X. X.; Zhou, Z. P.; Zhang, R. X.; Yan, Y. S. *J. Hazard Mater.* **2012**, *205*, 179.
28. Sambe, H.; Hoshina, K.; Moaddel, R.; Wainer, I. W.; Haginaka, J. *J. Chromatogr. A* **2006**, *1134*, 88.
29. Longo, L.; Scorrano, S.; Vasapollo, G. *J. Polym. Res.* **2010**, *17*, 683.
30. Lai, J. P.; Lu, X. Y.; Lu, C. Y.; Ju, H. F.; He, X. W. *Anal. Chim. Acta* **2001**, *442*, 105.
31. Kan, X. W.; Zhao, Q.; Zhang, Z.; Wang, Z. L.; Zhu, J. *J. Talanta* **2008**, *75*, 22.
32. Beltran, A.; Marcé, R. M.; Cormack, P. A. G.; Borrull, F. *J. Chromatogr. A* **2009**, *1216*, 2248.
33. Boonpangrak, S.; Prachayasittikul, V.; Bülow, L.; Ye, L. *J. Appl. Polym. Sci.* **2006**, *99*, 1390.
34. Phutthawong, N.; Pattarawarapan, M. *J. Appl. Polym. Sci.* **2013**, *128*, 3893.
35. Summers, G. J.; Maseko, R. B.; Summers, C. A. *Eur. Polym. J.* **2013**, *49*, 1111.
36. Semsarzadeh, M. A.; Mirzaei, A.; Vasheghani-Farahani, E.; Haghighi, M. N. *Eur. Polym. J.* **2003**, *39*, 2193.
37. Vaughan, A. D.; Sizemore, S. P.; Byrne, M. E. *Polymer* **2007**, *48*, 81.
38. Yang, W. M.; Cao, Y.; Xu, X. L.; Zhou, Z. P.; Liu, L. K.; Xu, W. Z. *J. Mater. Res.* **2013**, *28*, 2666.
39. Wang, G.; Zhu, X. L.; Cheng, Z. P.; Zhu, J. *Eur. Polym. J.* **2003**, *39*, 2161.
40. Lu, C. Y.; Zhou, N. L.; Xiao, Y. H.; Tang, Y. D.; Jin, S. X.; Wu, Y.; Shen, J. *Appl. Surf. Sci.* **2013**, *264*, 36–44.
41. Xu, L. C.; Pan, J. M.; Dai, J. D.; Li, X. X.; Hang, H.; Cao, Z. J.; Yan, Y. S. *J. Hazard Mater.* **2012**, *233*, 48.
42. Yang, Y. Z.; Liu, X.G.; Guo, M. C.; Li, S.; Liu, W. F.; Xu, B. S. *Colloid Surf. A: Physicochem. Eng. Asp.* **2011**, *377*, 379.
43. Lopez, C.; Claude, B.; Morin, Ph.; Max, G. P.; Pena, R.; Ribet, J. P. *Anal. Chim. Acta* **2011**, *683*, 198.
44. Fouda, I. M.; Oraby, A. H.; Seisa, E. A. *J. Appl. Polym. Sci.* **2010**, *118*, 1306–1312.
45. Al-Rashed, S. M.; Al-Gaid, A. A. *J. Saudi Chem. Soc.* **2012**, *16*, 209.
46. Nityanandi, D.; Subbhuraam, C. V. *J. Hazard Mater.* **2009**, *170*, 876.
47. Wu, F. C.; Tseng, R. L.; Juang, R. S. *Chem. Eng. J.* **2009**, *150*, 366.
48. Akpa, O. M.; Unuabonah, E. I. *Desalination* **2011**, *272*, 20.